Instrument Science Report WFPC2 2010-05

WFPC2 Filters after 16 Years on Orbit

P. L. Lim[1], M. Quijada[2], S. Baggett[1], J. Biretta[1], J. MacKenty[1], R. Boucarut[2], S. Rice[2], and J. del Hoyo[2,3]

December 14, 2010

ABSTRACT

In a joint investigation by GSFC and STScI, the Selectable Optical Filter Assembly (SOFA) of WFPC2 was extracted and the filter wheels removed and examined for any on-orbit changes. The filters were inspected, photographed and scanned with a spectrophotometer at GSFC. The data have been analyzed at STScI with a view towards understanding how prolonged exposure to the HST space environment affected the filters and what the resultant impacts are to WFPC2 calibrations.

We summarize our results from these post-SM4 laboratory studies, including a comparison of pre- to post-mission filter throughput measurements, evaluations of the UV filter red leaks, and assessment of the condition of the filter coatings.

1. Introduction

WFPC2 was installed on HST in December 1993 during SM1 by the crew of Shuttle Mission STS-61. WFPC2 replaced WF/PC-1, providing improved UV performance, more advanced detectors, better contamination control, and its own corrective optics. After 16

[1] Space Telescope Science Institute, Baltimore, MD
[2] Goddard Space Flight Center, Greenbelt, MD
[3] University of Arizona, Tucson, AZ

years of exceptional service, WFPC2 was retired in May 2009 during SM4, when it was removed from HST in order to allow for the installation of WFC3.

During the 16-year WFPC2 mission, over 185,000 exposures were taken (~135,000 science and the rest calibration), all of which are now public and available from the STScI Archive[4]. When WFPC2 was brought back to the ground, we took the opportunity to study its filters that had been exposed to the space environment for more than a decade and use the results to improve science calibrations.

The main goal is to look for changes in filter transmissions or bandpass wavelengths, if any. Due to resource limitations, we only scanned 33 out of the 48 filters. We selected the filters of interest by prioritizing them according to usage, wavelength coverage, etc. The selected elements are tabulated in Table 1. The filters chosen for post-mission scanning are those with known on-orbit changes, high and regular utilizations, UV filters for which we wish to check the red leak, and other reasons, such as unique manufacturing technology (e.g., F160AW, F160BW, and quad filters) or anomaly seen during inspection.

We discussed preliminary results for F160AW, F160BW, F170W, F343N, and F450W in Lim et al. (2010), which is superseded by this report where disagreements exist. Analysis, results, and summary are presented in Sections 2, 3, and 4, respectively.

Table 1: WFPC2 filters chosen for lab scanning.

Category	Filters
Known on-orbit changes	F122M[a], F160BW[b], F343N[c]
High utilization	F300W, F450W, F555W, F606W, F675W, F702W, F814W, F850LP
Regular utilization	F255W, F336W, F439W, F502N, F656N, F658N, F673N
UV filters[d]	F170W, F185W, F218W
Others[e]	F130LP, F160AW, F165LP, F375N, F380W, F390N, F437N, F467M, F469N, F487N, F1042M, FQUVN

[a] Biretta & Gonzaga (2008, private communication); Lim et al. (2009).
[b] Biretta & Verner (2009).
[c] Gonzaga & Biretta (2009).
[d] Red leak only.
[e] Included based on lab inspection, etc.

2. Analysis

All 12 wheels were removed from the SOFA for inspection and scanning at GSFC by M. Quijada and J. del Hoyo. Follow-up analysis was primarily done at STScI. Cosmetic inspections to look for surface features (e.g., stains, spots, and pinholes) were performed

[4] http://archive.stsci.edu/hst/search.php

in April, July, and August 2010 by J. MacKenty, S. Baggett, J. Biretta, P. L. Lim, M. Quijada, and J. Trauger. Such features might or might not affect the filter transmissions.

For scanning, we used a commercial off-the-shelf spectrophotometer with a parallel double-beam monochromator. This differential beam measurement enabled us to infer filter transmissions from a non-vacuum lab environment as on-orbit performance. This method is most likely similar to pre-launch measurements at JPL (Holtzman et al. 1995); though this cannot be confirmed due to the lack of pre-launch literature. Later on-orbit adjustments only involved simple transmission rescaling (see Section 3). Therefore, the fact that the lab setup did not match on-orbit *f*-ratio or beam size is not an issue.

The procedure was performed at room temperature (~25°C), which was slightly warmer than on-orbit (~12-14°C). For WFC3 filters, wavelength shifts due to temperature differences were estimated to be no more than 0.07Å/°C (Baggett 2010, private communication). Assuming the WFPC2 filters behave in a similar fashion to the later-generation WFC3 filters, the worst case WFPC2 filter, with bandwidth ~20Å (McMaster et al. 2008), would experience a wavelength change of ~5%. We note that this assumption might not hold given the different heritage between WFPC2 and WFC3 filters, particularly in the aspects of manufacturing technology and space exposure; but unfortunately this is the best comparison available due to the lack of WFPC2 pre-launch scanning information.

Due to UV absorption by atmospheric O_2, we were unable to obtain good signal-to-noise for wavelengths less than ~2000Å. The scanner wavelength resolution ranged from ~0.5-50Å. We deemed it sufficient to use higher resolution for in-band transmissions and lower for out-of-band. The lower limit of measurable transmission is ~10^{-6}-10^{-8}.

To study spatial homogeneity, we scanned a filter at different locations, as illustrated in Figure 1. For square filters (all scanned except F160AW, F160BW, and FQUVN) – center, top left, top right, bottom left, and bottom right; round filters (F160AW and F160BW) – center, top, bottom, left, and right; and the redshifted [OII] quad filter (FQUVN) – center of each quadrant. These locations are defined for a filter that is sitting at the bottom of its wheel standing on the rim, with the smooth side (as opposed to the clamp side) facing the incoming beam at right angle. We note that for Wheels 1-11, it was the clamp side that actually faced the incoming beam in HST, which could not be replicated due to equipment constraint. However, this would not affect our results as the transmittance that we measured is an invariant quantity that does not depend on the direction of the incident light.

Figure 1: Scanned filter locations shown in red for: **(a)** square filters; **(b)** round filters, i.e., F160AW and F160BW; and **(c)** redshifted [OII] quad filter, i.e., FQUVN. WFPC2 CCDs are superimposed on the filter field-of-view, as given in WFPC2 Instrument Handbook (McMaster et al. 2008). Diagrams on the left are approximately to-scale with actual dimensions. Examples of each filter shape are shown on the right.

(a)

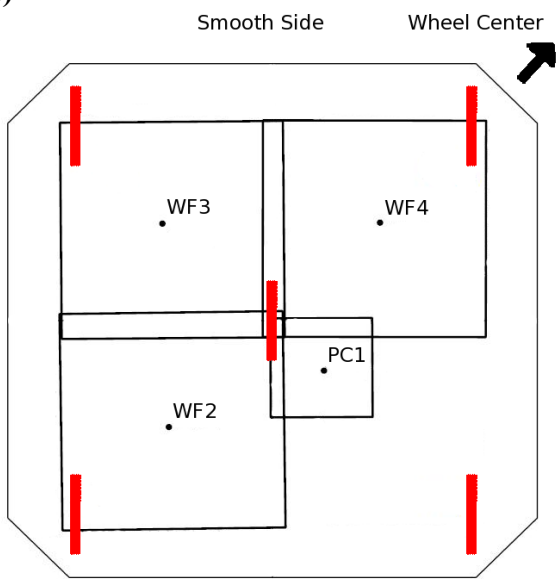

Example: F122M

(b)

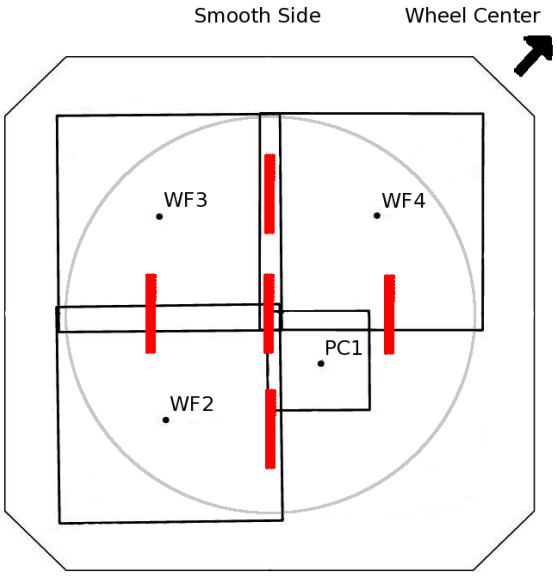

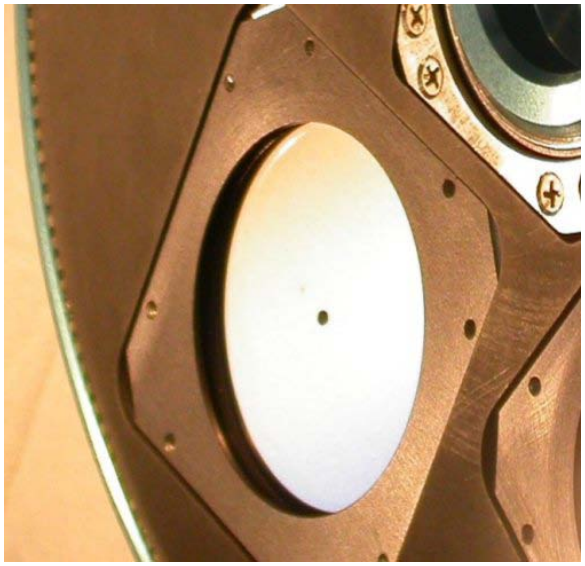

Example: F160AW

(c)

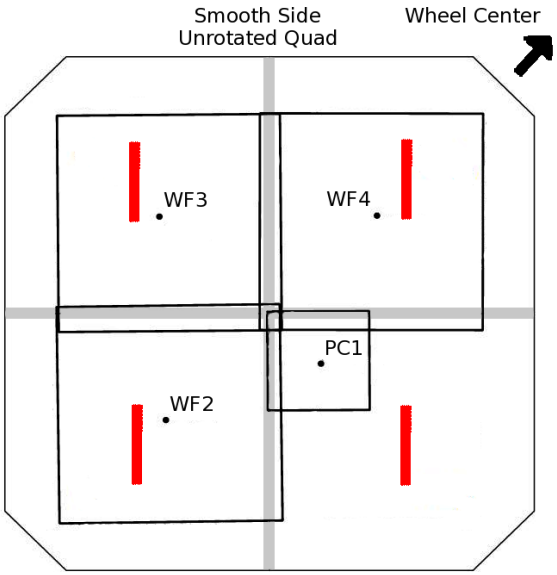

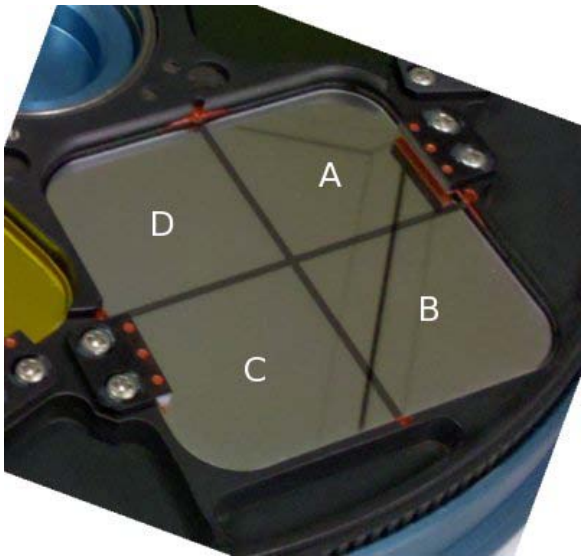

Example: FQUVN (clamp side shown; flip horizontally for smooth side orientation)

3. Results

We compared the scanned transmission curves (hereafter, post-flight) with pre- and in-flight data. Pre-flight is defined as the first version of CDBS filter transmission curves[5], which was taken in the lab prior to the WFPC2 mission. In-flight is the latest version used during the WFPC2 mission, mostly adjusted by Baggett et al. (1997) based on on-orbit photometric calibrations, which is also publicly available from CDBS[5]. The post-flight results are available on the WFPC2 webpage[6] via FTP[7]. For further reference, pre-flight WFPC2 optical filters specification by JPL is also available on WFPC2 webpage[8].

For the in-band regions, we find that some post-flight filter transmission curves agree better with the pre-flight filter curves than they do with the in-flight curves. However, this does not necessarily mean that the component itself physically changed between ground to orbit or vice versa; the filter curve change may simply be a calibration artifact. The filter transmission curves, along with other components (HST OTA, WFPC2 optics, QE, etc.), are used in SYNPHOT to provide calibration information for science images (e.g., PHOTFLAM with sensitivity value). Pre-launch SYNPHOT baseline was derived during ground tests, which was later optimized using on-orbit spectrophotometric observations to adjust for filter and QE transmission curves (Baggett et al. 1997).

[5] ftp://ftp.stsci.edu/cdbs/comp/wfpc2/
[6] http://www.stsci.edu/hst/wfpc2/analysis/filters.html
[7] ftp://ftp.stsci.edu/instrument_news/WFPC2/filterscans/
[8] http://www.stsci.edu/hst/wfpc2/documents/filters.pdf

It is plausible that the cause for the change between ground and on-orbit photometry lies elsewhere along the HST optical path or even within the ground test equipment instead of the adjusted elements. Since SYNPHOT uses a convolution of all optical elements to calibrate science images, this does not affect existing WFPC2 calibrations. The post-flight transmission scans *cannot* be used in conjunction with the other current optical elements in SYNPHOT. Investigation of other elements in the optical path is beyond the scope of this project.

Post-flight data show that a majority of the broadband, medium-band, and long-pass filters have not evolved within a few percent; whereas, narrowband filters are more sensitive to slight variations (i.e., the same absolute change is more significant in the latter). The significance of any observed filter change depends on the individual science application; hence, we will let the readers decide for themselves based on our quantitative comparisons whether the changes affect their science. We summarize our post-flight results in Table 2. Detailed inspections, measurements, and plots are available as downloadable files, as described in Section 3.1.

Table 2: Summary of post-flight results, with filters ordered by wheels and slots. The column % SCI is the percentage of total science exposures (datasets) using a given filter; Science exposures constitute ~73% of the total WFPC2 datasets. See Table 3.1 in WFPC2 Instrument Handbook (McMaster et al. 2008) for science applications of the filters.

Filter	Wheel	Slot	% SCI	Summary
F953N	1	1	0.91	Not scanned.
F160AW	1	2	0.00	Out-of-band shows significant inhomogeneities and increase in red leak from pre-flight. These changes are due to deteriorating sodium layers and pinhole growth[a]. This filter was not used on-orbit.
F160BW	1	3	0.94	Out-of-band is similar and below scanner limit for all scanned locations; consistent with observations (Lim et al. 2009). Pinhole growth reported by Biretta & Verner (2009) does not seem to affect our results.
F122M	1	4	0.33	Out-of-band is similar for all scanned locations. No in-band data possible in non-vacuum lab setup to confirm throughput drop reported by Biretta & Gonzaga (2008, private communication).
F130LP	2	1	0.26	All scanned locations agree within ~2%, with largest transmission variations around 7000Å. Both pre- and in-flight's resolutions are too low for useful qualitative comparisons.
F165LP	2	2	0.04	All scanned locations agree with each other and with both pre- and in-flight within ~2% (pre- and in-flight are identical).
F785LP	2	3	0.38	Not scanned.
F850LP	2	4	1.47	All scanned locations are identical. They agree better with pre- than in-flight. For $\lambda < 8000$Å, scanned transmission is the upper limit only.
F336W	3	1	2.78	All scanned locations are identical. In-band region agrees better with pre- than in-flight. Out-of-band agrees with both pre- and in-flight within respective detection limits.
F410M	3	2	0.79	Not scanned.

Filter	Wheel	Slot	% SCI	Summary
F467M	3	3	0.36	For in-band, all scanned locations agree within ~5% with each other, and agree better with pre- than in-flight. Out-of-band agrees with both pre- and in-flight within respective detection limits.
F547M	3	4	2.12	Not scanned.
F791W	4	1	0.74	Not scanned.
F569W	4	2	0.12	Not scanned.
F675W	4	3	2.88	For in-band, all scanned locations agree within ~2% with each other, and agree better with in-flight, which is almost identical to pre-flight. Out-of-band agrees with both pre- and in-flight within respective detection limits.
F439W	4	4	2.47	Surface smudge at center causes transmission difference of ~5-10% around 4000Å and 4600Å. The smudge was recorded in JPL's pre-flight report[a] and accounted for in pre-flight transmission. Other scanned locations for in-band are identical with each other. In-band, especially the center, agrees better with pre- than in-flight. Out-of-band agrees with both pre- and in-flight within respective detection limits.
F343N	5	1	0.10	For in-band, transmission variations are within ~10%. Significant changes in shape and transmission from in-flight are consistent with Gonzaga & Biretta (2009). Filter surface shows features that suggest deteriorating layers. For out-of-band, in which all measurements agree, no meaningful comparisons with pre- and in-flight were possible due to lack of data in the latter two.
F375N	5	2	0.17	For in-band, transmission variations are within ~10%, where lower left and right vary the most from the rest. "Diagonal" feature, which was also mentioned in JPL's pre-flight report[a], is seen on filter surface. For out-of-band, in which only upper limits are measured, no meaningful comparisons with pre- and in-flight were possible due to lack of data in the latter two.
F390N	5	3	0.10	For in-band, transmission variations are within ~10%. For all scanned locations, the peak transmissions are consistently higher than both pre- and in-flight by ~5%, with slight shape change around 3910Å. Out-of-band agrees with in-flight within respective detection limits (no meaningful data from pre-flight[b]).
F437N	5	4	0.08	For in-band, all scanned locations agree within ~2% except for the center, which varies by ~10% from the rest. Transmission shape has changed and overall peak wavelength is ~7Å redder than JPL[a] pre-, STScI pre-, and in-flight. Filter surface shows smudges and internal structures. Out-of-band agrees with in-flight within respective detection limits (no data from pre-flight[b]).
F469N	6	1	0.17	In-band lower left and right have a different shape (only single peak) than the rest. Ignoring lower left and right, peak wavelength is ~3Å redder and FWHM ~2Å narrower than existing data. Peak transmission agrees better with pre- than in-flight. Filter surface shows tiny features and a "trapezoid." For out-of-band, in which only upper limits are measured, no meaningful comparisons with pre- and in-flight were possible due to lack of data in the latter two.
F487N	6	2	0.18	For in-band, transmission variations are ~10%, with excess transmission around 4880Å for top left and right, and center. Overall transmission agrees better with pre- than in-flight. Filter surface has a "comet" and other features. Out-of-band agrees with in-flight within respective detection limits (no meaningful data

Filter	Wheel	Slot	% SCI	Summary
				from pre-flight[b]).
F502N	6	3	1.24	For in-band, transmission variations are within ~5%, except top and lower left, which have slight shape change and ~2Å redshift in peak wavelength. Overall transmission is between pre- and in-flight. Out-of-band shows some excess near in-band wings for lower right; Otherwise, it agrees with in-flight within respective detection limits (no meaningful data from pre-flight[b]).
F588N	6	4	0.17	Not scanned.
F631N	7	1	0.42	Not scanned.
F656N	7	2	2.41	For in-band, although FWHM and peak transmission variations are within ~5%, all locations have different shapes and peak wavelengths. Center and top left somewhat agree with pre-flight. Top and lower right are similar, whereas lower left looks like a mirror image of the former. Filter surface shows "comet" features. Out-of-band agrees with in-flight within respective detection limits (no meaningful data from pre-flight[b]).
F658N	7	3	0.97	For in-band, although FWHM and peak transmission variations are within ~10%, all locations have different shapes and peak wavelengths. Only top and lower right appear similar. None of them particularly agree with pre- or in-flight, but lower left shows the largest deviation. Filter surface has “a smudge or two.” Out-of-band agrees with in-flight within respective detection limits (no meaningful data from pre-flight[b]).
F673N	7	4	1.21	For in-band, only top left and right, and center are identical. Lower left and right have different shapes and peak wavelengths. None of them particularly agree with pre- or in-flight. Filter surface shows “growth" on one edge and dusts. Out-of-band agrees with in-flight within respective detection limits (no meaningful data from pre-flight[b]).
F170W	8	1	1.99	Out-of-band agrees for all scanned locations, and with both pre- and in-flight.
F185W	8	2	0.17	Out-of-band agrees for all scanned locations and with pre-flight. Its agreement with in-flight is reasonable considering that the latter was reconstructed empirically by Lim et al. (2009) using stellar observations.
F218W	8	3	0.89	For in-band, transmissions vary by ~10%. Peak wavelength is ~28Å redder and FWHM ~10Å wider than pre- and in-flight. Transmission is ~11% lower than in-flight, which is already less than pre-flight. Out-of-band agreement with in-flight is reasonable considering that the latter was also reconstructed by Lim et al. (2009) in a similar fashion as F185W.
F255W	8	4	1.18	For in-band, transmissions vary by ~10% and fall between pre- and in-flight. Out-of-band shape shows some variations from in-flight, which was also reconstructed by Lim et al. (2009). Transmission at $\lambda > 8500$Å shows upper limit only.
F380W	9	1	0.16	For in-band, all scanned locations agree within ~5% with each other, and agree with both pre- and in-flight (the latter two are identical). Out-of-band agrees with in-flight within respective detection limits (no meaningful data from pre-flight[b]).
F555W	9	2	11.45	For in-band, all scanned locations are identical, and agree with both pre- and in-flight (the latter two are identical). Out-of-band agrees with both pre- and in-flight within respective detection limits.

Filter	Wheel	Slot	% SCI	Summary
F622W	9	3	0.22	Not scanned.
F300W	9	4	9.25	For in-band, all scanned locations agree within ~5%. Overall transmission agrees better with pre- than in-flight; although peak wavelength is ~20Å redder and FWHM is ~25Å wider. Filter surface shows a smudge and some "dots." Out-of-band agrees with both pre- and in-flight within respective detection limits.
F814W	10	1	19.69	For in-band, all scanned locations agree within ~3% with each other, and agree better with pre- than in-flight. Out-of-band agrees with both pre- and in-flight within respective detection limits.
F606W	10	2	21.04	For in-band, all scanned locations agree within ~5% with each other, and with both pre- and in-flight (the latter two are similar). However, one should take note of the variations of the narrow secondary peak around 7100Å. Out-of-band agrees with both pre- and in-flight within respective detection limits.
F702W	10	3	2.18	For in-band, all scanned locations agree within ~5%. Most notable variations are around 6000Å and 8000Å, especially for the center. Filter surface shows a smudge at the center, which was also mentioned in JPL's pre-flight report[a]. Overall transmission agrees with both pre- and in-flight (the latter two are similar). Out-of-band agrees with both pre- and in-flight within respective detection limits.
F450W	10	4	5.28	For in-band, all scanned locations are identical with each other, and agree with both pre- and in-flight (the latter two are similar). Out-of-band agrees with both pre- and in-flight within respective detection limits.
POLQ	11	1	1.02	Not scanned.
F1042M	11	2	0.92	For in-band, all scanned locations agree within ~2%, and agree better with pre- than in-flight. Peak wavelength is ~31Å redder than pre- and in-flight. Filter surface shows "watermark" in a corner. Out-of-band agrees with both pre- and in-flight within respective detection limits.
FQUVN	11	3	0.08	In-band is redshifted by 11Å, 15Å, 14Å, and 21Å for quads A, B, C, and D, respectively. FWHM increased the most in quad D, i.e., by 3Å. Peak transmission difference from in-flight is the largest in quad C, i.e., ~20% higher. Overall, quad A and D are the best and the worst, respectively. Filter surface shows lots of structures on all quads. Out-of-band has insufficient pre- and in-flight data for comparison.
FQCH4N	11	4	0.78	Not scanned.
FR418N	12	1	0.08	Not scanned.
FR533N	12	2	0.47	Not scanned.
FR680N	12	3	0.51	Not scanned.
FR868N	12	4	0.18	Not scanned.

[a] J. Trauger (2010, private communication).

[b] It is unclear why out-of-band data were missing from pre-flight or how they ended up in subsequent versions.

3.1. File descriptions

The files in this section are the detailed results that are summarized in Table 2. They are available for download via FTP[7].

A. **wfpc2_inspection_report.pdf** – Detailed visual inspection notes and photographs for all 12 wheels, regardless of whether the filters were scanned.

The following files are available for each scanned filter, where appropriate (i.e., some filters might not have some of the files). To look for the filter of interest, replace ***filter*** in the listed generic file name with the actual filter name (e.g., **f555w**). A slash (/) and an asterisk (*****) in the names denote sub-directory and wildcard, respectively.

B. ***filter*/*filter*_*quijada.txt** – Scanned transmissions for each location as stated in the file header on the first row (except FQUVN files that have no headers). Location order: square filters – center, top left, top right, lower left, and lower right; F160AW and F160BW – center, top, right, left, and bottom; FQUVN – center only (each quadrant is a separate file and identifiable from the file name). The first column is the wavelength, generally 1900Å to 20,000Å. Transmission files in CDBS[5] cover 1000Å to 11,000Å. Negative transmission values, especially in the out-of-band regions, are due to spurious scanner readings – discard them for throughput calculations. Below is an excerpt from **f300w_quijada.txt**:

```
# w(A)     Center         Top_L          Top_R          Low_L          Low_R
1900.0      5.67000E-06   -3.26200E-05    4.11200E-05     3.40300E-05     7.23200E-05
1950.0     -5.61000E-06    1.40000E-06    2.81000E-06    -1.12200E-05     2.66500E-05
   …            …              …              …              …              …
25000.0    -2.99000E-05   -3.68700E-05    1.00000E-06    -6.57700E-05    -5.48100E-05
```

C. ***filter*/wfpc2_*filter*_new_syn.txt** – Averaged values from ***filter*_*quijada.txt** above. This file follows a similar format as the ASCII filter throughput files in CDBS[5], i.e., no header, and with wavelength (Å) and transmission in the first and second columns, respectively. FQUVN's equivalent of this are the **fquvn_*quijada.txt** as described above. Below is an excerpt from **wfpc2_f300w_new_syn.txt**:

```
1900.0      2.41040E-05
1950.0      2.80600E-06
   …            …
25000.0    -3.72700E-05
```

D. ***filter*/wfpc2_*filter*_redleak_syn.txt** – This is similar to **wfpc2_*filter*_new_syn.txt** above but only contains the red leak regime for UV filters that have in-band situated blue-ward of 2000Å, i.e., F122M, F130LP, F160AW, F160BW, F165LP, F170W, and F185W.

E. ***filter*/plots/*filter*_*trans*.png** – Plots of transmission vs. wavelength for each scanned location or the average, with or without comparisons to pre- and in-flight, as stated in the plot legends. Files ending in **inband.png**, **outband1.png**, **outband2.png**, and **outband.png** show in-band, out-of-band for blue leak region, out-of-band for red leak region, and out-of-band for either region (when only one of them exists for the filter), respectively. When neither **inband** nor **outband** is stated, the whole wavelength range is shown. Out-of-band plots that appear noisy

are likely to represent transmission upper limits only due to scanner limitations. An example is shown in Figure 2 for F300W in-band region.

F. ***filter*/plots/*filter*_*syn_*num**.png** – Plots showing measurements of peak wavelength, peak transmission, FWHM, half-max transmission, and half-max wavelengths on both sides. The placeholder ***num*** denotes a number (e.g., **001**). For pre-flight – ***num*** is always **001**; in-flight – same as the latest version in CDBS[5]; post-flight – in-flight plus one. Post-flight measurements are done for center (***num*_cen.png**), top left (***num*_topl.png**), top right (***num*_topr.png**), lower left (***num*_lowl.png**), lower right (***num*_lowr.png**), and the average (***num*.png**). An example is shown in Figure 3 for F300W post-flight center scan.

The following file is only available for F343N. It is the same as Figure 3 in Lim et al. (2010).

G. **f343n/plots/f343n_compare_0304.png** – Similar to Figure 1 in Gonzaga & Biretta (2009) but with post-flight filter transmission comparison also added. The plot shows the ratio of observed to predicted fluxes over time. Standard star observations using PC1 and WF3 are shown as filled circles and crosses, respectively. Blue and red data points compare the observations to the in- and post-flight filter transmission curves, respectively. Ratio of 1 indicates that the observations agree with the predictions.

The following files are only available for F437N.

H. **f437n/wfpc2_f437n_jpl_inband.txt** – Pre-flight transmission obtained from JPL (J. Trauger 2010, private communication) that is different from STScI pre-flight data for unknown reasons. The columns are wavelength (Å) and transmission, respectively. Only in-band region is available.

I. **f437n/plots/f437n_syn_jpl.png** – Similar to ***filter*_*syn_*num**.png** above and contains measurements for **wfpc2_f437n_jpl_inband.txt**.

We summarize the available files by filter in Table 3. If a file is found to be unexpectedly missing from FTP[7], please contact STScI Help Desk[9].

[9] help@stsci.edu, (410) 338 1082, or (1 800) 544 8125

Figure 2: An example for FTP file category E mentioned in Section 3.1. This is a plot of F300W in-band transmission across wavelength for pre-flight, in-flight, and each of the scanned post-flight locations, as indicated by the legend. This file is available for download from FTP[7] as `f300w/plots/f300w_trans_inband.png`.

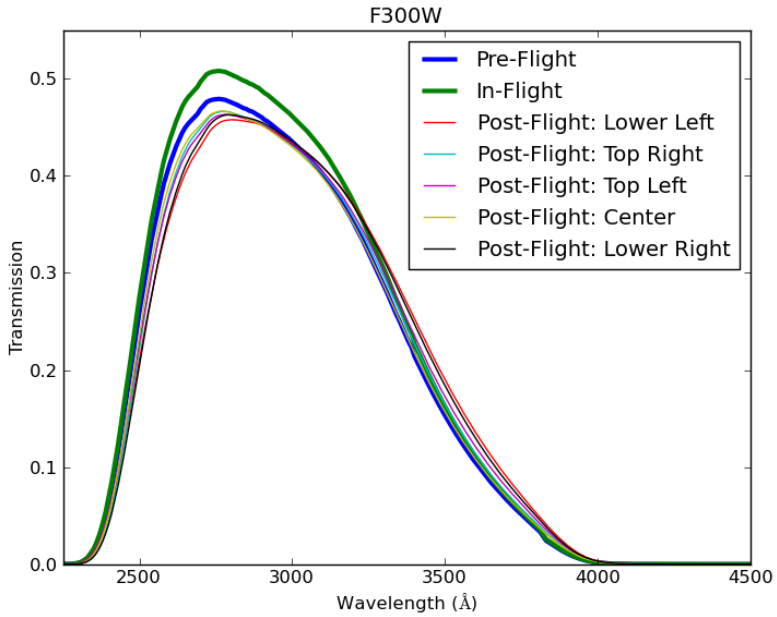

Figure 3: An example for FTP file category F mentioned in Section 3.1. This is a plot of F300W in-band transmission curve measurements for post-flight scan at the center of the filter. Values for peak wavelength, peak transmission, FWHM, half-max transmission, and half-max wavelengths on both sides are shown. This file is available for download from FTP[7] as `f300w/plots/f300w_syn_007_cen.png`.

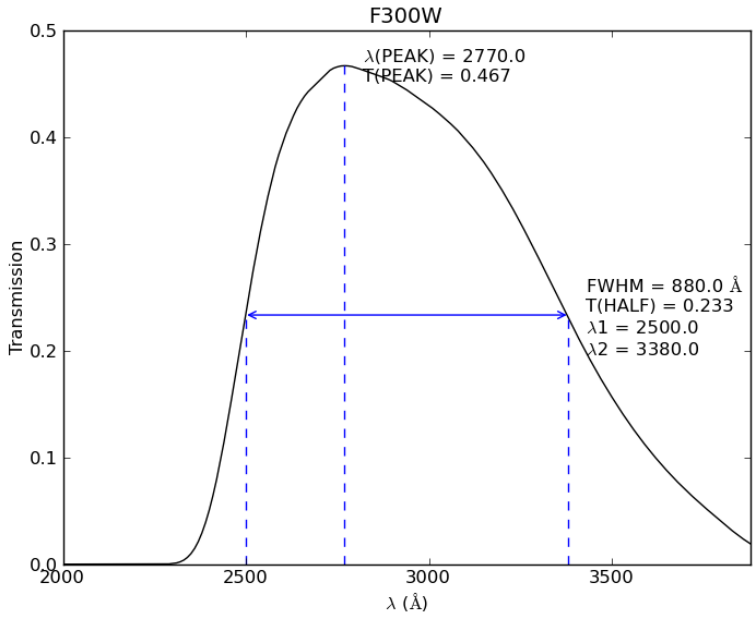

Table 3: File availability by filter. Each file category is represented by its alphabet, as listed in Section 3.1. A check mark (✓) denotes that the filter has file(s) in the given category.

Filter	Wheel	Slot	A	B	C	D	E	F	G	H	I
F953N	1	1	✓								
F160AW	1	2	✓	✓		✓	✓				
F160BW	1	3	✓	✓		✓	✓				
F122M	1	4	✓	✓		✓	✓				
F130LP	2	1	✓	✓		✓	✓				
F165LP	2	2	✓	✓		✓	✓				
F785LP	2	3	✓								
F850LP	2	4	✓	✓	✓		✓				
F336W	3	1	✓	✓	✓		✓				
F410M	3	2	✓								
F467M	3	3	✓	✓	✓		✓				
F547M	3	4	✓								
F791W	4	1	✓								
F569W	4	2	✓								
F675W	4	3	✓	✓	✓		✓				
F439W	4	4	✓	✓	✓		✓				
F343N	5	1	✓	✓	✓		✓	✓	✓		
F375N	5	2	✓	✓	✓		✓	✓			
F390N	5	3	✓	✓	✓		✓				
F437N	5	4	✓	✓	✓		✓	✓		✓	✓
F469N	6	1	✓	✓	✓		✓	✓			
F487N	6	2	✓	✓	✓		✓	✓			
F502N	6	3	✓	✓	✓		✓				
F588N	6	4	✓								
F631N	7	1	✓								
F656N	7	2	✓	✓	✓		✓	✓			
F658N	7	3	✓	✓	✓		✓	✓			
F673N	7	4	✓	✓	✓		✓	✓			
F170W	8	1	✓	✓		✓	✓				
F185W	8	2	✓	✓		✓	✓				
F218W	8	3	✓	✓	✓		✓	✓			
F255W	8	4	✓	✓	✓		✓				
F380W	9	1	✓	✓	✓		✓				
F555W	9	2	✓	✓	✓		✓				
F622W	9	3	✓								
F300W	9	4	✓	✓	✓		✓	✓			
F814W	10	1	✓	✓	✓		✓				
F606W	10	2	✓	✓	✓		✓				
F702W	10	3	✓	✓	✓		✓				
F450W	10	4	✓	✓	✓		✓				
POLQ	11	1	✓								
F1042M	11	2	✓	✓	✓		✓				
FQUVN	11	3	✓	✓			✓	✓			
FQCH4N	11	4	✓								
FR418N	12	1	✓								
FR533N	12	2	✓								
FR680N	12	3	✓								
FR868N	12	4	✓								

4. Summary

Given the 16 years of significant and unprecedented WFPC2 contributions to the scientific community and the nearly 200,000 WFPC2 images in the MAST archives, it is imperative that we study its filters flown back from orbit during SM4 in order to improve science calibrations.

We inspected the filter surfaces for all elements in all 12 wheels in the SOFA and recorded the observed features, which might or might not affect the transmissions. We scanned 33 out of the 48 filters at multiple locations to assess inhomogeneities. Unlike their in-flight counterparts, the post-flight filter throughputs do not account for any evolution in other HST optical elements; hence, the post-flight scans should *not* be used as-is in the current SYNPHOT for WFPC2 as they might not provide the proper calibration.

We presented a summary of the results by filter and made the corresponding data files available for download on the WFPC2 webpage. Most filters, except narrowband, remain stable to within a few percent. Some filters, especially narrowbands, show inhomogeneities or changes, which might or might not be significant depending on individual science goals.

Follow-up analyses left as future work include investigating the possible causes for the changes observed in the filters, using the post-flight filter transmission curves to derive an update for the SYNPHOT calibrations, and vacuum-level scanning of the in-band sections of the UV filters.

Acknowledgements

We would like to thank Dr. John Trauger (JPL) for sharing his valuable expertise on WFPC2 filters and Dr. Kenneth Sembach for HST Mission Office approvals. We are also grateful to Dr. Ralph Bohlin, Dr. David Golimowski, and Amber Armstrong who provided useful feedback.

References

Baggett, S., Casertano, S., Gonzaga, S., & Ritchie, C. 1997, WFPC2 Synphot Update, WFPC2 ISR 1997-10

Biretta, J. & Verner, K. 2009, Rapid Pinhole Growth in the F160BW Filter, WFPC2 ISR 2009-01

Gonzaga, S. & Biretta, J. 2009, WFPC2 F343N Filter Throughput Decline, WFPC2 ISR 2009-02

Holtzman, J. A., Burrows, C. J., Casertano, S., Hester, J. J., Trauger, J. T., Watson, A. M., & Worthey, G. 1995, PASP, 107, 1065

Lim, P. L., Chiaberge, M., Biretta, J., & Di Nino, D. 2009, Red Leak Characterization for the WFPC2 UV Filters, WFPC2 ISR 2009-07

Lim, P. L., Quijada, M., Baggett, S., Biretta, J., MacKenty, J., Boucarut, R., Rice, S., & del Hoyo, J. 2010, in 2010 HST Calibration Workshop, ed. S. Deustua & C. Oliveira (Baltimore, MD: STScI), in press

McMaster, M., Biretta, J., et al. 2008, WFPC2 Instrument Handbook, Version 10.0 (Baltimore: STScI)